MoS$_2$ materials synthesized on SiO$_2$/Si substrates via MBE

Linjie Zhan[‡], Wen Wan[‡], Zhenwei Zhu[‡], Tien-Mo Shih[‡], and Weiwei Cai[‡*]

[‡] Department of Physics, State Key Laboratory of Physical Chemistry of Solid Surfaces, Xiamen University, 361005, China

*Email: wwcai@xmu.edu.cn

Abstract. Two-dimensional (2D) MoS$_2$ materials possess indirect-to-direct bandgap tunability, and have enjoyed wide applications in electronics and optoelectronics. Most of investigators have ubiquitously synthesized these materials by using the chemical vaporization deposition (CVD) method. Here we have adopted MoO$_3$ source materials to synthesize MoS$_2$ on 280-nm SiO$_2$/Si substrates via molecular beam epitaxy (MBE). We have obtained triangular nucleation, tens-of-micron domain, and monolayer MoS$_2$. This MBE technique can be applied to synthesizing other members of semiconducting layered transition metal dichalcogenides (TMDCs), such as WS$_2$, MoSe$_2$, and WSe$_2$ materials.

1. Introduction

Layered TMDCs [1-3] have recently attracted great interest because of their specific optical and electronic properties. Within this class of 2D materials, MoS$_2$ possesses high in-plane mobility [4], large Seebeck coefficient [5], compatible nanopores [6], having enjoyed wide applications in electronics and optoelectronicsis [7-11]. Similarly as graphene films [12], MoS$_2$ films can be physically exfoliated from the bulk. However, generally the process requires much labor, yields low repeatability, and cannot conveniently produce entirely uniform monolayers. Additionally, CVD method has been widely used, and is capable of conveniently synthesizing deposited materials based on the nucleation mechanism. Sources of bulky quantities must be injected into the vacuumed tube, and are deposited on the substrate under relatively high temperatures. During this method, the sulfurization of MoO$_3$ jointly with CVD method is being commonly used. An approach for synthesizing MoS$_2$ flakes in rhomboid shapes with controllable number of layers by the layer-by-layer sulfurization of MoO$_2$ microcrystals [13] has also been developed with high-crystallinity domains occupying tens of microns. However, how to controllably prepare high-quality uniform monolayer MoS$_2$ films for the practical application of MoS$_2$ in electronics and optoelectronics has so far remained challenging.
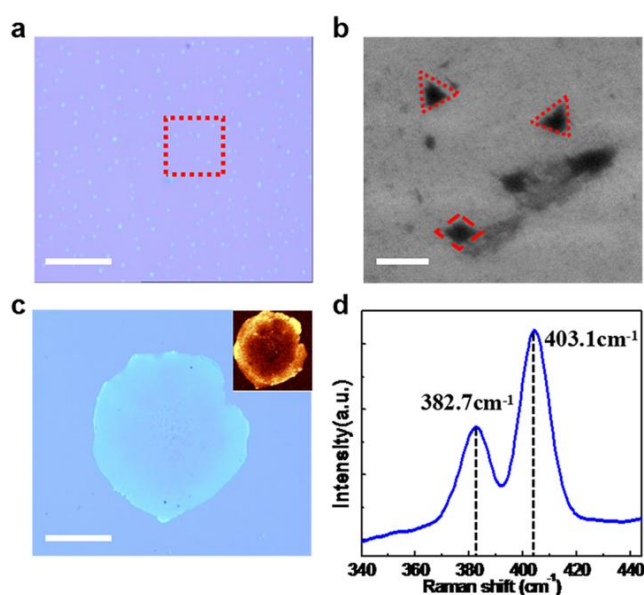
In comparison, first, MBE demands higher-degreed vacuum, leading to less contamination. Second, the substrate tends to be heated to low temperatures such that numbers of thermal-stress-induced wrinkles and cracks in the crystal structure decrease. Third, materials tend to be slowly synthesized, facilitating the control of crystal-structure accuracies. Finally, the MBE is capable of maneuvering intermittent syntheses, which allow impromptu changes of source materials in order to regulate epitaxial compositions and impurities. Consequently, the MBE technology widens the low-dimension-material research horizon. Here we have adopted MoO$_3$ source materials to synthesize MoS$_2$ on 280-nm SiO$_2$/Si substrates via MBE. Addition, we have obtained triangular nucleation, tens-of-micron domain and monolayer MoS$_2$. This MBE technique can be aptly applied to synthesizing other members of TMDCs and their heterojunctions.

2. MoS$_2$ materials synthesized on SiO$_2$/Si substrates
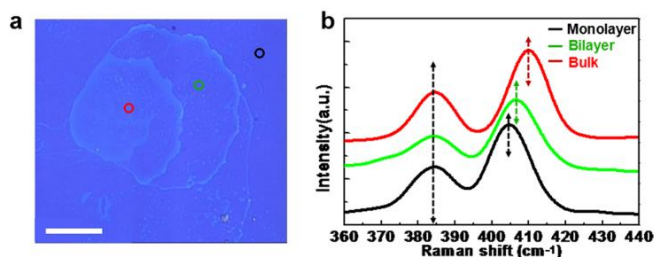
2.1. The nucleation and further growing of MoS$_2$

Owing to the reflection-enhancing effect on specific wavelengths of visible light between MoS_2 and 280-nm thick SiO_2 oxide layer on Si, MoS_2 layers can be observed by an optical microscope. Figure 1a shows the optical image of MoS_2 domains, and can be enlarged by the scanning electron microscopy (Figure 1b). Some domains look like triangles, indicating that MoS_2 crystallites possess a good crystallinity; some exhibit rhomboidal shapes [14], implying that crystals have not been fully sulfurized. When the grown time is extended, MoS_2 crystallites can be enlarged to tens of micron, which can be characterized by Raman spectrum, as shown in Figure 1c. The Raman spectrum of larger MoS_2 domain, shown in Figure 1d, is characterized by the Raman shift of E_{2g}^1 and A_{1g} modes lying in 382.7 and 403.1 cm^{-1}. The frequency difference between the E_{2g}^1 and A_{1g} modes is 20.4 cm^{-1}, confirming that the MoS_2 domain is monolayer.

Figure 1. The nucleation and further growing of MoS_2. (a) Optical image showing the nucleation of MoS_2 on SiO_2/Si. Scale bar, 20 μm. (b) Enlarged SEM image of the area indicated in the red dashed line in (a). Scale bar, 2 μm. (c) Optical image of MoS_2 in large domain. The inset shows Raman mapping of characteristic E_{2g}^1 peak (d) The Raman spectrum of MoS_2 in (c), showing the E_{2g}^1 and the A_{1g} peaks.
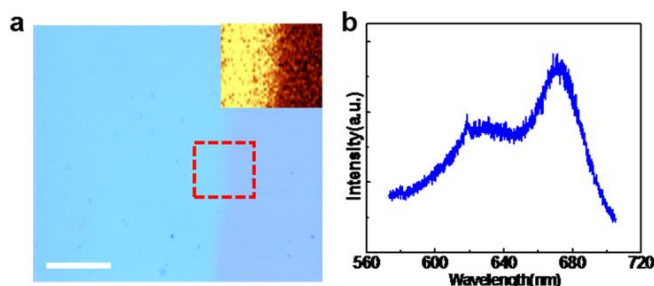
A conspicuous spiral-like MoS_2 domain is depicted in Figure 2a, of which the monolayer, bilayer, and bulk are represented by black, green, and read circles, respectively. In Figure 2b, Raman spectra of these circled MoS_2 are shown. Their E_{2g}^1 Raman-shift peaks are located almost at the same position (384.6 cm^{-1}), whereas A_{1g} counterparts are correspondingly situated at 404.6, 406.4, and 410.1 cm^{-1}. Frequency differences between E_{2g}^1 and A_{1g} peaks approximately equal 20.0, 21.8, and 25.5 cm^{-1} for monolayer, bilayer, and bulk MoS_2, respectively.

Figure 2. Spiral-like MoS_2 domain. (a) Optical image of spiral-like MoS_2 domain. Scale bar, 20 μm. (b) The Raman spectrum of corresponding area in (a).

2.2. Monolayer MoS2 in large scale

Large-scale monolayer MoS_2 has been readily prepared by our own lab-built MBE instrument, simply by extending the growing time to three hours or even longer. Figure 3a shows the optical image of SiO_2/Si substrate that is covered with monolayer MoS_2. Raman mapping (the intensity integration of A_{1g} peak) of edges, marked with the red dashed line, is shown in the inset, indicting a high uniformity of monolayer MoS_2. For the purpose of confirming the thickness, monolayer MoS_2 on SiO_2/Si is further investigated with photoluminescence spectroscopy (PL) measurements. The PL is a useful technique for readily distinguishing the thickness of MoS_2 material. At room temperature, the PL emission of monolayer MoS_2 lies typically between 1.82 and 1.89 eV [15]. The PL spectrum measured at room temperature (Figure 3b) shows two strong energy emission peaks at 1.84 eV (672 nm) and 2.01 eV (616 nm) which are regarded as the signature of monolayer MoS_2.

Figure 3. Monolayer MoS_2 in large scale. (a) Optical image of monolayer MoS_2. Inset: Raman mapping of the area indicated in the red dashed line. Scale bar, 60 μm. (b) Photoluminescence spectra of monolayer MoS_2.

3. Conclusion

In summary, we have synthesized triangular nucleation, tens-of-micron domain, and monolayer MoS_2 on 280-nm SiO_2/Si in the present study. Characterizations of the atomically-thin film using optical microscopes, Raman spectroscopy, and PL spectroscopy provide the evidence that morphology, layer thickness, optical properties, and electrical properties of the synthesized MoS_2 material bear the quality similar to those of the exfoliated monolayer MoS_2. As a controllable approach, the MBE technique enables us to study the nucleation and to further synthesize MoS_2 materials in large-scaled areas. It can be suitably applied to studying syntheses of other members of TMDCs and their heterojunctions.

References
[1]   E. del Corro et al., Nano Lett. 2016, **16,** 2363.
[2]   Y. W. Zhang et al., Appl. Phys. Lett. 2016, **108,** 153114.
[3]   H. Liu et al., ACS Nano 2015, **9,** 6619.
[4]   W. Z. Bao, X. H. Cai, D. Kim, K. Sridhara, and M. S. Fuhrer, Appl. Phys. Lett. 2013, **102,** 042104.
[5]   M. Buscema et al., Nano Lett. 2013, **13,** 358.
[6]   K. Liu, J. D. Feng, A. Kis, and A. Radenovic, ACS Nano 2014, **8,** 2504.
[7]   Q. Ji et al., Nano Lett. 2013, **13,** 3870.
[8]   Y. Gong et al., Nature Mater. 2014, **13,** 1135.
[9]   B. Radisavljevic, A. Radenovic, J. Brivio, V. Giacometti, and A. Kis, Nature Nanotechnol. 2011,**6,** 147.
[10]   A. Rezk et al., Nano Lett. 2016, **16,** 849.
[11]   W. Wan et al., *RSC Adv*. 2016, **6,** 323.
[12]   A. K. Geim, and K. S. Novoselov, Nature Mater. 2007, **6,** 183.
[13]   X. S. Wang, H. B. Feng, Y. M. Wu, and L. Y. Jiao, J. Am. Chem. Soc. 2013, **135,** 5304.

[14] Y. M. Shi et al., Nano Lett. 2012, **12,** 2784.

[15] K. M. McCreary et al., Adv. Funct. Mater. 2014,**41,** 6449.